Beitr. Phys. Atmosph., August 1995, p. 249–261
0005-8173/03 0249–13 $ 3.00/0

The Barotropic Dynamics of Tropical Cyclone Motion in a Large-Scale Deformation Field

by A. B. KRAUS[1], R. K. SMITH[2] and W. ULRICH

Meteorological Institute, University of Munich, Munich, Germany
[1]Current affiliation: Institut für Chemie und Dynamik der Geosphäre, 52425 Jülich, Germany
[2]Corresponding author's address: Prof. Roger K. Smith, Meteorological Institute, University of Munich, Theresienstr. 37, 80333 Munich, Germany

(Manuscript received January 31, 1995; accepted May 11, 1995)

Abstract

A numerical and analytic study of tropical-cyclone motion in a meridionally- and zonally-varying large-scale flow is presented. The numerical calculations are based on a barotropic model developed by the last author, while the analytic theory is an extension of that developed by the second author for the motion of a barotropic vortex in a zonal shear flow on a beta-plane. The analytic theory, though inaccurate for long term integrations of the equations, enables the principal effects of vortex motion in a general large-scale flow to be identified and quantified. It provides also a framework for interpreting the numerical calculations. Calculations are presented for a particular large-scale flow represented by a stationary, finite-amplitude Rossby wave with meridional wavenumber-two, in which there is substantial stretching deformation as well as vorticity. An important new finding is that, in the presence of strong stretching deformation, locations occur within the large-scale flow where the subsequent vortex motion is sensitive to the initial vortex position. Knowledge about the existence of such regions is relevant to the initialization of tropical cyclones in numerical prediction models, and to the question of the predictability of cyclone tracks. On account of the vorticity asymmetry associated with the large-scale absolute vorticity gradient, the locations of enhanced sensitivity do not lie along the axis of contraction of the deformation field as would happen if the vortex motion were associated with pure advection by the large-scale flow. Nor do they lie in regions where the Laplacian of the large-scale absolute vorticity is positive as conjectured by DeMaria. The implication is that, at least for the present flow, the sensitivity suggested by DeMaria is a higher-order effect, a conclusion that is supported by the analytic theory.

Zusammenfassung

Es wird eine numerische und analytische Untersuchung der Bewegung von tropischen Zyklonen in einer meridional und zonal veränderlichen Strömung vorgestellt. Die numerischen Rechnungen basieren auf einem barotropen Modell, das vom letzten der Autoren entwickelt wurde, während die analytische Theorie eine Erweiterung der Theorie des zweiten Autors ist, die die Bewegung eines barotropen Wirbels in einer Scherströmung auf der Beta-Ebene beschreibt. Die analytische Theorie, obgleich ungenau für längere Zeiträume, ermöglicht die Identifikation der Hauptursachen der Wirbelbewegung in einer allgemeinen, großskaligen Strömung, sowie die Abschätzung der einzelnen Beiträge. Sie stellt auch einen Rahmen für die Interpretation von numerischen Rechnungen zur Verfügung. Eine spezielle großskalige Strömung wird betrachtet, nämlich eine stationäre Rossby-Welle endlicher Amplitude mit meridionaler Wellenzahl zwei. Eine solche Strömung enthält sowohl beträchtliche Dehnungsverformung als auch Vorticity. Eine wichtige neue Erkenntnis ist, daß es bei starker Dehnungsdeformation Gebiete innerhalb der großskaligen Strömung gibt, in denen die weitere Bewegung des Wirbels sehr empfindlich auf eine kleine Verschiebung der Anfangsposition reagiert. Das Wissen um die Existenz solcher Gebiete ist sowohl für die Initialisierung von tropischen Zyklonen in numerischen Vorhersagemodellen, als auch für die Möglichkeiten der Vorhersagbarkeit tropischer Zyklonenbahnen von Bedeutung. Aufgrund der aus dem großskaligen Gradienten der absoluten Vorticity resultierenden Vorticityasymmetrie liegen die Orte erhöhter Empfindlichkeit nicht längs der Kontraktionsachse des Deformationsfeldes, wie es der Fall wäre, wenn die Wirbelbewegung allein durch Advektion durch die großskalige Strömung hervorgerufen würde. Sie liegen auch nicht in Gebieten, in denen der Laplace-Operator der großskaligen absoluten Vorticity positiv ist, wie von DeMaria vermutet. Daraus folgt, daß, zumindest für die untersuchte Strömung, der von DeMaria vorgeschlagene Effekt von höherer Ordnung ist. Diese Schlußfolgerung wird auch durch die analytische Theorie gestützt.

1 Introduction

Our current understanding of the dynamics of tropical cyclone motion has evolved largely from studies of barotropic vortex motion on a beta-plane. A brief review is given by Smith (1993). The prototype problem considers the motion of an initially symmetric vortex on a beta-plane in the absence of a large-scale flow. Numerical studies of this problem have been carried out by Chan and Williams (1987), Fiorino and Elsberry (1989), Smith et al. (1990, henceforth SUD) and Shapiro and Ooyama (1990). These studies highlighted the importance of a developing asymmetric flow component on the vortex motion. This flow component is associated with a relative vorticity asymmetry that is generated by the advection of planetary vorticity by the vortex circulation. The flow asymmetry has the form of a pair of counter-rotating gyres, the so-called beta-gyres. The asymmetric flow across the vortex centre, lying between the gyres, determines the north-westward component of the vortex motion to a good first approximation (Fiorino and Elsberry, 1989; SUD).

Further insight into the prototype problem was obtained from an analytic theory worked out by Smith and Ulrich (1990). The theory leads to an approximate solution of the nondivergent barotropic vorticity equation on a beta-plane and adopts a method of partitioning of the total flow into 'the vortex' and 'the environment' that was suggested by Kasahara and Platzman (1963). In this method, 'the vortex' is taken to be the initial symmetric vortex, suitably relocated, and 'the environment' is defined as the residual flow, i.e., the developing asymmetric flow field. The analytic theory was extended by Smith (1991, henceforth S91) and Smith and Weber (1993, henceforth SW93) to investigate the effect of a meridionally-varying zonal shear flow on the vortex motion. In this case, a three-way partitioning was adopted in which 'the environment' was further subdivided into 'the initially-imposed environment' (i.e. the shear flow) and the residual flow which characterizes 'the vortex asymmetry'.

In general, the large-scale environment of a tropical cyclone has a meridional as well as a zonal flow component and both of these components are functions of the zonal *and* meridional position. In other words, the flow has stretching deformation in addition to shearing deformation, vorticity, and divergence. It is important, therefore, to understand the additional effects of stretching deformation on the dynamics of vortex motion, a problem of relevance to the initialization of tropical cyclones in numerical forecast models.

In the present study, a series of calculations is presented for vortices initialized in a particular environmental flow in which there is substantial stretching deformation as well as vorticity. This initially-imposed environment is represented by a stationary Rossby wave with meridional wavenumber-two. Particular interest is focussed on the subsequent motion of vortices initialized at and around the point of maximum deformation within this flow. To the extent that vortices are advected by the large-scale flow, one might expect their subsequent motion to be sensitive to their initial position if it lies near the axis of contraction of the deformation field. This sensitivity is explored and it is shown that the region where it is most apparent is influenced by the large-scale absolute vorticity gradient. A hypothesis of DeMaria (1985) is examined also. He conjectured that a sensitivity of the subsequent track to initial vortex positions should arise in regions where the Laplacian of the large-scale absolute vorticity gradient is positive.

The availability of the analytic theory enables the principal effects of non-uniform shear and deformation to be isolated and quantified. The accuracy of the theory is indicated by comparing the results obtained with corresponding numerical solutions.

2 The Large-Scale Deformation Field

A suitable analytic expression for a stationary deformation field on a middle-latitude beta-plane centred at 12.5 deg is provided by the solution of the nondivergent barotropic vorticity equation for a stationary finite-amplitude Rossby wave with meridional wavenumber-two. In a frame of reference (x, y), fixed on the rotating earth with the x-axis pointing eastwards and the y-axis pointing northwards, the streamfunction $\hat{\psi}$ of such a wave is given by

$$\overline{\psi}(x) = \hat{\psi} \sin kx \sin ky - \hat{U} y, \qquad (1)$$

where $k = 2\pi\lambda^{-1}$ denotes the zonal and meridional wavenumber and λ is the corresponding wavelength. The associated velocity field $\overline{\mathbf{v}} = (u, v)$ is given by $\overline{\mathbf{v}} = \mathbf{k} \wedge \nabla \overline{\psi}$, where $\mathbf{k}$ denotes the vertical unit vector, and the vorticity is given by $\overline{\zeta} = \nabla^2 \overline{\psi}$. The constant $\hat{\psi}$ determines the maximum amplitudes $\overline{v}_{max}$ and $\overline{\zeta}_{max}$ of the background meridional velocity and vorticity fields, respectively. The constant background flow $\hat{U}$ is chosen as $0.5\,\beta\,k^{-2}$ to

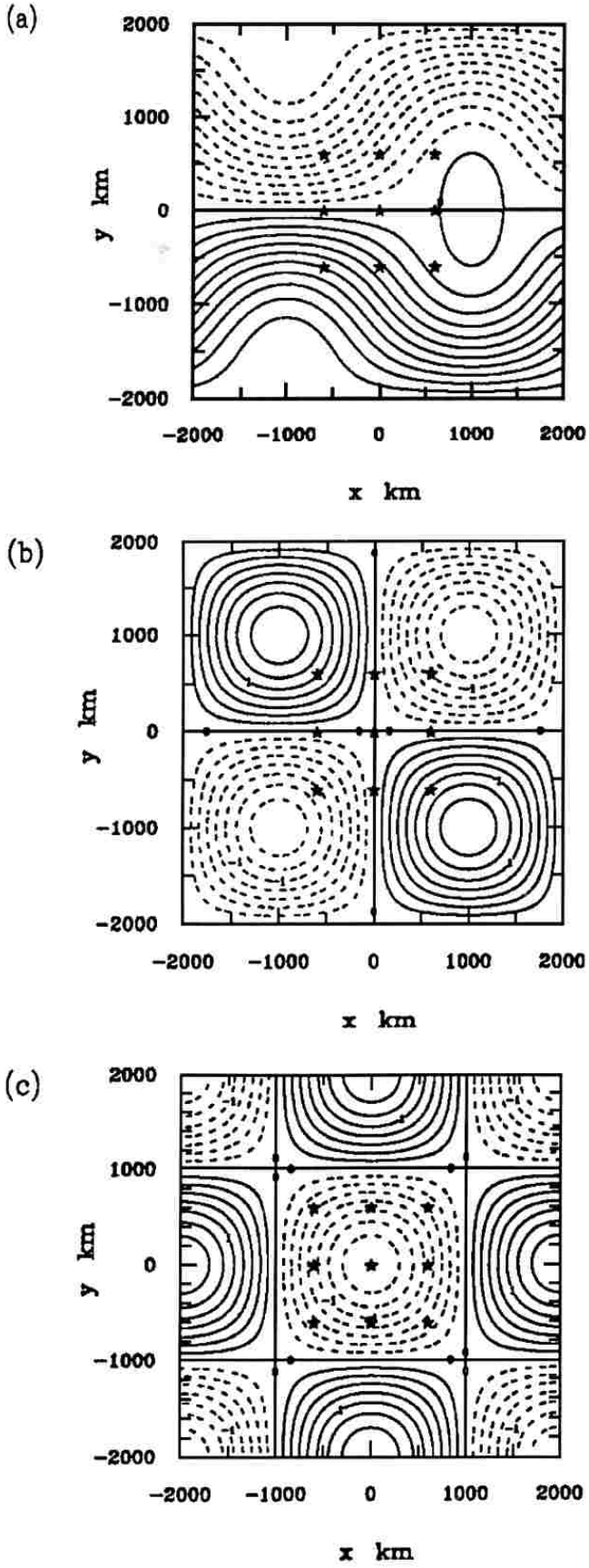

Figure 1 (a) Streamfunction, (b) vorticity, and (c) stretching deformation of the large-scale deformation field defined by Eq. (1) with $\lambda = 4000$ km, $\overline{v}_{max} = 5\ ms^{-1}$ and $\widehat{U} = 4.27\ ms^{-1}$. Contour intervals are $8 \times 10^5\ m^2\ s^{-1}$ in (a) and $2 \times 10^{-6}\ s^{-1}$ in (b) and (c). The nine stars in each panel denote the positions at which the symmetric vortex is initialized to calculate the subsequent vortex tracks.

ensure a zero phase velocity of the Rossby wave. In the calculations that follow, λ is taken as 4000 km and $\overline{v}_{max}$ as $5\ ms^{-1}$, whereupon $\overline{U} = 4.27\ ms^{-1}$. The structure of this large-scale deformation field is shown in Figure 1. The nine stars give the positions at which the symmetric vortex is situated at the initial time $t = 0$. The initial vortex positions are referred to by their location relative to the centre of the deformation field, i.e., SW for the initial vortex position in the southwest, WW for the one in the west, etc. At the centre position the absolute vorticity gradient reduces to β. The vortex initialized at that point is denoted by SU.

3 Numerical Model Integrations

The numerical model calculations were performed using a version of the barotropic model developed by SUD. The computational domain is a square $-L \le x, y \le L$, where $L = 2000$ km. Channel boundary conditions $v = \partial\psi/\partial x = 0$ are applied at $y = \pm L$ and periodic boundary conditions applied at $x = \pm L$. The grid resolution is 20 km in both the zonal and meridional direction. Other details can be found in Ulrich and Smith (1991). Since the vortex vorticity is confined predominantly to a domain of 500 km around the vortex centre and, for the most part, the vortex centres lie further than 500–1000 km from the nearest boundary, the motions of interest should be largely uncontaminated by the model boundaries. This enables us to make comparisons between the numerical model calculation and the corresponding analytic solution, even though different boundary conditions are used in the two formulations.

4 The Analytic Theory

The analytic method follows closely that developed by SW93 and will be sketched only briefly. The nondivergent barotropic vorticity equation is developed in a frame of reference (X, Y) moving with the vortex centre, the centre being defined as the location of the relative vorticity maximum. In this frame, the total horizontal wind vector and the vertical component of the relative vorticity are $\mathbf{u}_{tot}$ and $\zeta_{tot} = \mathbf{k} \cdot \nabla \wedge \mathbf{u}_{tot}$, respectively. Moreover, the Coriolis parameter f, varies both with latitude and with time t. The vortex centre position relative to a coordinate system (x, y) fixed at the initial centre position is denoted by $\mathbf{x}_c = (x_c(t), y_c(t))$, and the

vortex velocity in the fixed frame is $\mathbf{c}(t) = d\mathbf{x}_c/dt = (c_1(t), c_2(t))$.

As in SW93, the Kasahara-Platzman Method III of partitioning is adopted in which the total flow is decomposed into 'the vortex' and 'the environment'. The vortex is defined as the initial symmetric vortex suitably relocated and is denoted by the index "v". The environment consists of two parts: the stationary Rossby wave, i.e., the environmental flow at the initial time, denoted by an overbar; and the residual flow, denoted by a prime. The residual flow is obtained by subtracting the vortex and the initially imposed large-scale flow from the total flow. Replacing $\mathbf{u}_{tot}$ by $\mathbf{u}_v + \overline{\mathbf{u}} + \mathbf{u}'$ and ζ_{tot} by $\zeta_v + \overline{\zeta} + \zeta'$, the barotropic vorticity equation can be written as the sum of three equations for $\partial\zeta_v/\partial t$, $\partial\overline{\zeta}/\partial t$, and $\partial\zeta'/\partial t$. The equation for $\partial\zeta_v/\partial t$ is satisfied trivially, because $\mathbf{u}_v \cdot \nabla\zeta_v = 0$ in the moving frame. The equation for $\partial\overline{\zeta}/\partial t$, which must be satisfied in the absence of a vortex, can be left in the fixed frame, (x, y). Then, the equation for $\overline{\zeta}$ is satisfied by the stationary Rossby wave solution represented by Eq. (1). Therefore, it remains only to consider the equation for ζ', i.e.,

$$\frac{\partial\zeta'}{\partial t} + \mathbf{u}_v \cdot \nabla(\zeta' + \overline{\zeta} + f) = - \mathbf{u}' \cdot \nabla(\zeta_v + \zeta' + \overline{\zeta} + f) - \overline{\mathbf{u}} \cdot \nabla(\zeta_v + \zeta'). \quad (2)$$

An approximate analytic solution of Eq. (2) may be obtained iteratively as described by Smith and Ulrich (1990) and S91. Recently, SW93 showed that for the case of an initially symmetric vortex superimposed on a large-scale zonal shear flow, the iterative procedure can be derived from a scale analysis. A key assumption is that the absolute vorticity gradient $B_* \equiv |\nabla(\overline{\zeta} + f)|$ of the large-scale flow is slowly varying on the scale of the vortex. The variables representing the residual flow are expanded in terms of a single dimensionless parameter $\varepsilon \equiv B_* L^2 U^{-1}$, where L and U are suitable length and velocity scales and B_* denotes the value of $|\nabla(\overline{\zeta} + f)|$ at the initial vortex centre position. A similar expansion parameter was introduced by Peng and Williams (1990) for the case of a quiescent environment.

When interest is focused on the vortex motion, the vortex length and velocity scales L and U should be chosen in a way that they characterize the outer part of the symmetric vortex profile where the vorticity asymmetry ζ' has coherent structure (Fiorino and Elsberry, 1989; SUD). SW93 chose for the 'broader vortex' they studied, L = 300 km, the radius beyond which the tangential wind is below gale-force ($U = 15\ ms^{-1}$). As the same vortex profile is used here, the same values for L and U are adopted. The vortex vorticity ζ_v is assumed to scale with UL^{-1}. The gradient of the vortex vorticity, $d\zeta_v/dr$ varies by more than two orders of magnitude on the scale of the vortex and again, an appropriate scale for this is one which is characteristic for the region where the vorticity asymmetry is coherent. Taking B_* as a scale for $d\zeta_v/dr$ tends to be an underestimate, while UL^{-1} tends to be an overestimate, although not by an order of magnitude. Here we adopt the former choice because it leads to a considerable simplification of the algebra.

In the present problem, the basic-state absolute vorticity gradient $|\nabla(\overline{\zeta} + f)|$ depends on the vortex position relative to the centre of the large-scale deformation field. Despite the significant variation of B_* on the scale of the large-scale flow, the spatial variation of $|\nabla(\overline{\zeta} + f)|$ over the vortex scale is less than 15 % for any initial position. Accordingly, $|\nabla(\overline{\zeta} + f)|$ is assumed to be slowly varying over the scale of the vortex. The values of B_* as well as those of ε are listed in Table 1 for the nine initial vortex positions investigated. The largest value of ε occurs at the initial vortex position WW, where B_* is largest. Similarly, ε is smallest east of the deformation field centre (position EE), where the large-scale vorticity gradient nearly cancels β. Table 1 shows also the locally-defined velocity scale U_e of the deformation field.

Table 1 Scale of the absolute vorticity gradient $B_* \equiv |\nabla(\overline{\zeta} + f)|$, dimensionless parameter ε and scale of the environmental flow $U_e \equiv |\overline{\mathbf{u}}|$ for the nine initial vortex positions defined in Section 2.

	SW, NW	WW	SS, NN	SU	SE, NE	EE
$B_* \times 10^{11}\ m^{-1}\ s^{-1}$	3.29	4.11	2.12	2.12	0.94	0.12
ε	0.21	0.25	0.17	0.13	0.09	≤ 0.01
$U_e\ ms^{-1}$	7.07	8.33	5.89	4.29	3.05	0.24

Inserting $(\mathbf{u}', \zeta') = \varepsilon(\mathbf{u}_1', \zeta_1') + \varepsilon^2(\mathbf{u}_2', \zeta_2') + \cdots$ into Eq. (2) leads to a set of differential equations for the vorticity asymmetry at each order of ε:

$$\frac{d_v \zeta_1'}{dt} = -\mathbf{u}_v \cdot \nabla(\overline{\zeta} + f) \tag{3}$$

$$\frac{d_v \zeta_2'}{dt} = -\mathbf{u}_1' \cdot \nabla(\zeta_v + \overline{\zeta} + f + \zeta_1') - \overline{\mathbf{u}} \cdot \nabla(\zeta_v + \zeta_1') \tag{4}$$

$$\frac{d_v \zeta_3'}{dt} = -\mathbf{u}_2' \cdot \nabla(\zeta_v + \cdots) \tag{5}$$

where the operator $d_v/dt \equiv \partial/\partial t + \mathbf{u}_v \cdot \nabla$ denotes differentiation following hypothetical air parcels moving in circular paths around the vortex centre.

Ulrich and Smith (1991) showed that in the fixed frame of reference, the vortex motion $\mathbf{c}(t)$ can be attributed to the total environmental flow across the vortex centre to a good first approximation. Thus, $\mathbf{c}(t)$ is taken as $\overline{\mathbf{v}}(\mathbf{x_c}) + \mathbf{c}'(t)$, where $\overline{\mathbf{v}}(\mathbf{x_c})$ and $\mathbf{c}'(t)$ denote the flow components at the vortex centre associated with the large-scale flow and with the vortex asymmetry, respectively. The component $\mathbf{c}'(t)$ consists of the sum of contributions $\mathbf{c}_1'(t)$, $\mathbf{c}_2'(t), \cdots$ which are calculated step-by-step from the corresponding vorticity asymmetry $\zeta_1', \zeta_2', \cdots$. Thereby, each contribution $\mathbf{c}_n'(t)$, $n = 1, 2, \ldots$ is determined by solving the Poisson equation $\nabla^2 \psi_n' = \zeta_n'$ with the boundary condition

$$\lim_{|\mathbf{X}| \to \infty} \mathbf{u}_n'(\mathbf{X}, t) = -\mathbf{c}_n'(t). \tag{6}$$

and the subsidiary constraint

$$\mathbf{u}_n'(\mathbf{0}, t) = \mathbf{k} \wedge \nabla \psi_n'\big|_{\mathbf{X} = \mathbf{0}} = \mathbf{0}. \tag{7}$$

Together, Eqs. (6) and (7) provide the necessary closure assumption for the analytic theory.

In the moving frame of reference, the large-scale flow is obtained from that specified in the fixed frame using a Taylor-series expansion about the initial vortex position $\mathbf{x_0} = (x_0, y_0)$, see Appendix, Eq. (A1). This approximation is valid provided that the large-scale flow is slowly varying on the scale of the vortex displacements. Then the environmental absolute vorticity may be approximated by

$$\overline{\zeta} + f = (\overline{\zeta} + f)\big|_{\mathbf{x} = \mathbf{x_0}} + A(X + x_c) + B(Y + y_c),$$

where

$$(A, B) = \left(\frac{\partial \overline{\zeta}}{\partial x}, \frac{\partial(\overline{\zeta} + f)}{\partial y}\right)\Bigg|_{\mathbf{x} = \mathbf{x_0}} =$$

$$(-2\widehat{\psi} \cos kx_0 \sin ky_0, -2\widehat{\psi} \sin kx_0 \cos ky_0 + \beta).$$

Since $\mathbf{x_c} = O(\varepsilon)$, the terms associated with the temporal rate-of-change of $\overline{\zeta} + f$, i.e., $\partial(\overline{\zeta} + f)/\partial t = Ac_1 + Bc_2$, must be included on the right-hand side of Eq. (4).

Following S91, the solution of Eq. (3) is

$$\zeta_1'(r, \theta, t) = \zeta_{1c}'(r, t) \cos \tilde{\theta} + \zeta_{1s}'(r, t) \sin \tilde{\theta}, \tag{8}$$

where, $(\zeta_{1c}'(r, t), \zeta_{1s}'(r, t)) = -B_* r [\sin(\Omega t), 1 - \cos(\Omega t)]$, $\Omega = \Omega(r) = V(r)/r$, $B_* = \sqrt{(A^2 + B^2)}$, $\tilde{\theta} = \theta + \theta_*$, and

$$\theta_* = \tan^{-1}(A/B). \tag{9}$$

The first-order asymmetric streamfunction ψ_1' is obtained by solving the Poisson equation $\nabla^2 \psi_1' = \zeta_1'$, subject to the conditions (6) and (7), a calculation that can be performed analytically (see S91, Eq. (3.8)). The corresponding first-order asymmetric velocity field is given by $\mathbf{u}_1' = \mathbf{k} \wedge \nabla \psi_1'$. The first-order contribution $\mathbf{x}_{c1}'(t)$ to the vortex track is calculated as in S91, Section 6.[1] The contribution to the total vortex velocity $\mathbf{c}(t)$ that arises from $\overline{\mathbf{v}}(\mathbf{x_c})$ is calculated using a time interval t of one hour.

At this stage, Eq. (4) is solvable for the second-order vorticity asymmetry. Being linear in ζ_2', this equation can be decomposed into the sum of five separate equations each of which may be integrated with respect to time. The five equations are

- $\frac{d_v}{dt} \zeta_{21}' = -\mathbf{u}_1' \cdot \nabla \zeta_v$, which represents the advection of the symmetric vortex vorticity by the first-order asymmetric flow,
- $\frac{d_v}{dt} \zeta_{22}' = -\mathbf{u}_1' \cdot \nabla(\overline{\zeta} + f) - Ac_1 - Bc_2$, which represents the advection of the absolute vorticity by the first-order asymmetric flow,

[1] Equations (6.2) and (6.3) of S91 contain misprints. The correct form of these equations is

$$\begin{bmatrix} x_{c1}(t) \\ x_{c2}(t) \end{bmatrix} = \begin{bmatrix} \sin\theta_* & -\cos\theta_* \\ \cos\theta_* & \sin\theta_* \end{bmatrix} \begin{bmatrix} F_c \\ F_s \end{bmatrix},$$

where $F_n(t) = -\frac{1}{2} \int_0^t \int_0^\infty \zeta_{1n}'(\rho, \tau)\, d\rho\, d\tau$, and n denotes either of the indices c or s.

- $\frac{d_v}{dt}\zeta'_{23} = -\mathbf{u}'_1 \cdot \nabla\zeta'_1$, which represents the advection of the first-order asymmetric vorticity by the first-order asymmetric flow,
- $\frac{d_v}{dt}\zeta'_{24} = -\overline{\mathbf{u}} \cdot \nabla\zeta_v$, which represents the advection of the symmetric vortex vorticity by the initial environmental flow,
- $\frac{d_v}{dt}\zeta'_{25} = -\overline{\mathbf{u}} \cdot \nabla\zeta'_1$, which represents the advection of the asymmetric vortex vorticity by the initial environmental flow.

Expressions for the three contributions ζ'_{21}, ζ'_{22} and ζ'_{23} are given by S91, whereas the contributions ζ'_{24} and ζ'_{25} are derived here for the case of an environmental flow that varies both zonally and meridionally.

A general large-scale environmental flow may be decomposed locally into fields of pure divergence $\overline{D}$, pure rotation $\overline{\zeta}$, stretching deformation $\overline{E}$, and shearing deformation $\overline{F}$. The form of the operator $\overline{\mathbf{u}} \cdot \nabla$ in this case is given in the Appendix, Eq. (A2). In the special case of the deformation field given by Eq. (1), both $\overline{D}$ and $\overline{F}$ are equal to zero, together with their derivatives. The temporal rate-of-change of ζ'_{24} then reduces to

$$\begin{aligned}\frac{d_v\zeta'_{24}}{dt} &= -\overline{\mathbf{u}} \cdot \nabla\zeta'_{24} \\ &= -\left[\frac{r^2}{16}(\overline{E}_x - \overline{\zeta}_y)\cos\theta + \frac{r^2}{16}(\overline{\zeta}_x - \overline{E}_y)\sin\theta\right. \\ &\quad + \frac{r}{2}(\overline{E} + x_c\overline{E}_x + y_c\overline{E}_y)\cos 2\theta + \\ &\quad \left. + \frac{r^2}{8}\overline{E}_x\cos 3\theta + \frac{r^2}{8}\overline{E}_y\sin 3\theta\right]\frac{d\zeta_v}{dr}. \qquad (10)\end{aligned}$$

Eq. (10) is integrated with respect to time by replacing θ by $\theta + \Omega(r)\,t$ and resubstituting for θ after the integration has been carried out. The result is

$$\begin{aligned}\zeta'_{24}(r,\theta,t) &= \zeta'_{241c}(r,t)\cos\theta + \zeta'_{241s}(r,t)\sin\theta \\ &\quad + \zeta'_{242c}(r,t)\cos 2\theta + \zeta'_{242s}(r,t)\sin 2\theta \qquad (11) \\ &\quad + \zeta'_{243c}(r,t)\cos 3\theta + \zeta'_{243s}(r,t)\sin 3\theta\end{aligned}$$

where

$$\begin{bmatrix}\zeta'_{242c}(r,t)\\ \zeta'_{242c}(r,t)\end{bmatrix} = -\frac{r\overline{E}}{2\Omega}\frac{d\zeta_v}{dr}\begin{bmatrix}\sin(2\Omega t)\\ 1-\cos(2\Omega t)\end{bmatrix} + \begin{bmatrix}\zeta'_{242xc}(r,t)\\ \zeta'_{242xc}(r,t)\end{bmatrix}. \qquad (12)$$

Expressions for $\zeta'_{241n}(r,t)$, $\zeta'_{242xn}(r,t)$, and $\zeta'_{243n}(r,t)$, with n = "c" or "s", are given in the Appendix. The contribution to the second-order vorticity asymmetry arising from ζ'_{25} is rather complicated. It is given in Hellmeier (1993). The terms were calculated analytically using the Maple algebraic software, but, for the nine initial vortex positions investigated in the present study, the contribution of these terms to the total vortex displacement at 48 hours is less than 1 km.

5 Structure of the Vorticity Asymmetry

The contributions to the first-order and second-order vorticity asymmetry and their dependence on the flow parameters are summarized in Table 2. The symbols B_* and B_*^2 indicate that a particular wavenumber contribution has an amplitude proportional to the initial absolute vorticity gradient or its square, respectively. In the presence of an east-west basic-state absolute vorticity gradient, the patterns of these contributions are rotated, the rotation being clockwise for a basic-state absolute vorticity gradient pointing to the northeast or to the southwest and counterclockwise for one pointing to the northwest or to the southeast (see Eq. (9)). For the initital vortex positions considered here, the counterclockwise rotation of the first-order vorticity asymmetry is largest at the position NE where $\theta_* = 52°$. At the position SE, a clockwise rotation of the same angle occurs. The only asymmetric vorticity contribution that is independent of B_* is ζ'_{24}; this is determined by the advection of vortex vorticity by the large-scale flow.

(a) Effects of Horizontal Deformation

The most important contribution to the second-order asymmetric vorticity is from ζ'_{24}, which arises from the advection of vortex vorticity by the large-scale flow, and the most important contribution to ζ'_{24} itself is the wavenumber-two component ζ'_{242}. In the present flow configuration, all nine initial vortex positions are located in a region of negative stretching deformation ($\overline{E} < 0$) in which the velocity associated with the deformation field is distributed relative to the moving vortex centre as depicted schematically in Figure 2a. On the western side of the vortex centre, either the eastward flow component is stronger, or the westward flow component is weaker, than on the eastern side. Similarly, on the northern side of the vortex centre either the northward flow component is stronger, or the southward flow component is weaker, than on the southern side. Thus, at outer vortex radii ($r > 250$ km) where

Table 2 Summary of the terms contributing to the first-order and second-order vorticity asymmetry. Column 3 shows the azimuthal wavenumber contributions of each term; the meaning of wavenumber-zero is an axisymmetric contribution. The letters in Column 3 denote the origin of the corresponding contribution:

B_*: absolute vorticity gradient at the initial vortex position

E: stretching deformation $E \equiv \partial \overline{u}/\partial x - \partial \overline{v}/\partial y$ of the large-scale deformation field

E_x: spatial derivative of E

$\overline{\zeta}$: vorticity $\overline{\zeta} \equiv \partial \overline{v}/\partial x - \partial \overline{u}/\partial y$ of the large-scale deformation field

$\overline{\zeta}_x$: spatial derivative of $\overline{\zeta}$

Contribution to ζ'	Vorticity term	Wavenumber contributions 0	1	2	3	4
ζ'_1	$-\mathbf{u}_v \cdot \nabla(\overline{\zeta} + f)$		B_*			
ζ'_{21}	$-\mathbf{u}'_1 \cdot \nabla \zeta_v$		B_*			
ζ'_{22}	$-\mathbf{u}'_1 \cdot \nabla(\overline{\zeta} + f)$	B_*^2		B_*^2		
ζ'_{23}	$-\mathbf{u}'_1 \cdot \nabla \zeta'_1$	B_*^2		B_*^2		
ζ'_{24}	$-\overline{\mathbf{u}} \cdot \nabla \zeta_v$		$E_x\,\overline{\zeta}_x$	$E\,B_*^2$	$E_x\,\overline{\zeta}_x$	
ζ'_{25}	$-\overline{\mathbf{u}} \cdot \nabla \zeta'_1$	$B_*\,E_x\,\overline{\zeta}_x$	$B_*\,E\,\overline{\zeta}$	$B_*\,E_x\,\overline{\zeta}_x$	$B_*\,E_x$	$B_*\,E_x\,\overline{\zeta}_x$
ζ'_{26}	$-\mathbf{x}_c \cdot \nabla(\overline{\zeta} + f)$	B_*^2				

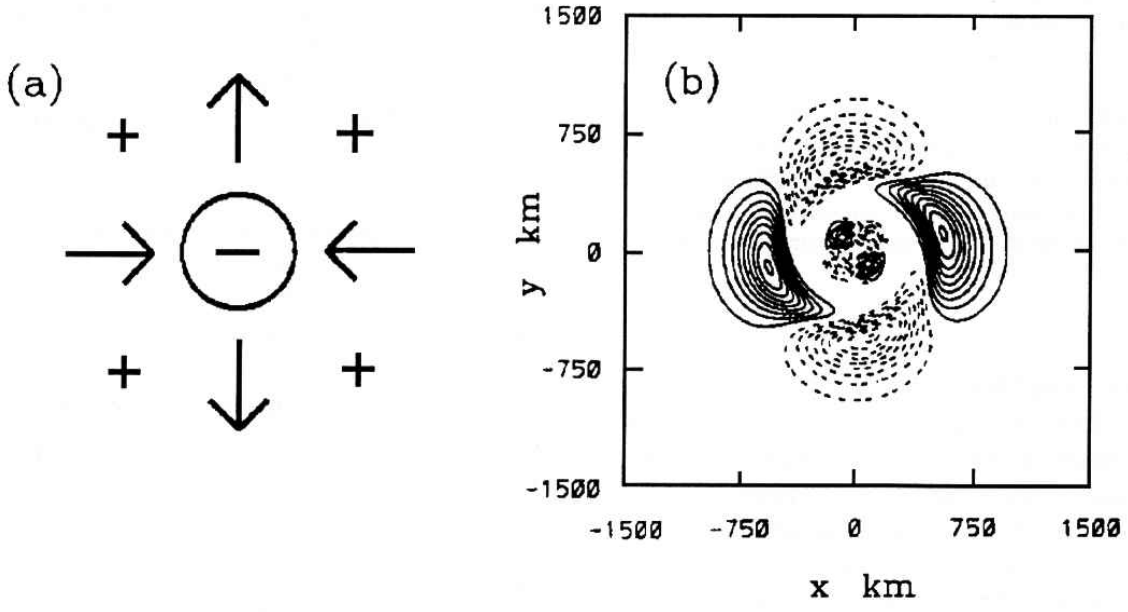

Figure 2 Schematic depiction of the wavenumber-two vorticity tendency arising from (a) the term $\overline{\mathbf{u}} \cdot \nabla \zeta_v$ and (b) the wavenumber-two component of ζ'_{24} for the initial vortex position SW after 24 hours. The minus sign in (a) denotes the region of positive vortex vorticity gradient $d\zeta_v/dr$. This region is separated from the region of negative vorticity gradient (plus signs) by the circle. Arrows denote the flow associated with the deformation field relative to the vortex centre. In (b), dashed lines indicate negative values and the contour interval is $2 \times 10^{-6}\,s^{-1}$. The vortex centre is at the centre of each panel.

$d\zeta_v/dr > 0$, there is positive vorticity advection towards the vortex centre in the zonal direction and negative vorticity advection in the meridional direction. In the inner part of the vortex, where $d\zeta_v/dr < 0$, the sign of the vorticity advection is reversed. In this region, however, the vorticity asymmetry is strongly sheared azimuthally. The vorticity pattern that emerges is characterized by ζ'_{242} and is shown in Figure 2b for the initial vortex position SW after 24 hours. The structure of ζ'_{242} is very similar to that shown in Figure 2b for the other initial positions.

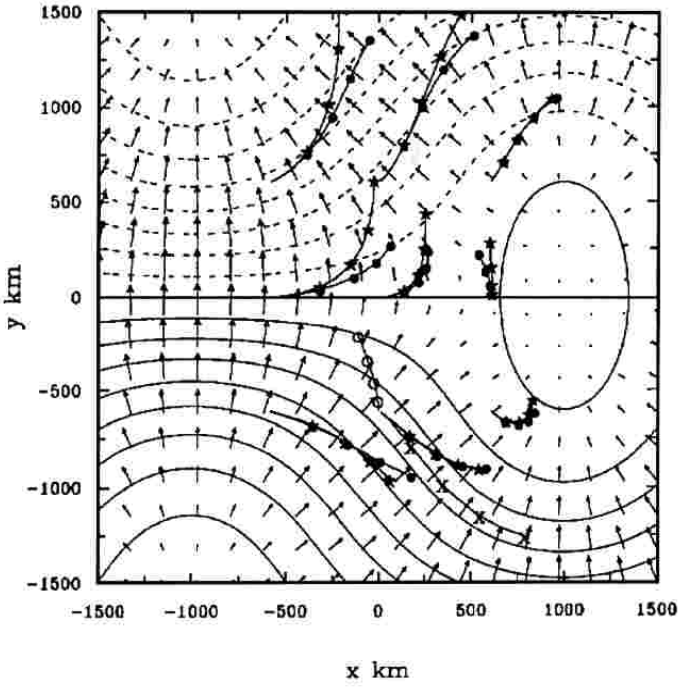

Figure 3 Vortex tracks calculated analytically (symbols *) and numerically (symbols •), where the symbols denote the vortex centre position every 12 hours. Solid (positive) and dashed lines (negative) are streamfunctions of the planetary-wave field; the contour interval is 1×10^6 m^2 s^{-1}. Small arrows represent the absolute vorticity gradient $\nabla(\bar{\zeta} + f)$, where the length of the vector is proportional to $|\nabla(\bar{\zeta} + f)|$. Additional tracks are shown starting at the initial vortex position SS. These are calculated from the components of the vortex motion which are associated with the developing vorticity asymmetries only (symbol ○) and assuming advection by the flow associated with the deformation field only (symbol X).

The maximum amplitude of the wavenumber-one and wavenumber-three components of ζ'_{24} are less than half as large as that of ζ'_{242} for the nine initial vortex positions investigated here. In particular, the flow across the vortex centre associated with the wavenumber-one contribution of ζ'_{24} is relatively small so that the effect of deformation on the vortex track is mostly indirect through its effect on the pattern of advection.

(b) Evolution of the Symmetric Circulation

In the method of partitioning adopted here, the vortex is defined to be the initial symmetric vortex, suitably located. Accordingly, the evolving symmetric vorticity components contained in ζ'_2 are regarded as part of the residual flow. The amplitudes of these components are locally small compared with the vorticity of the total residual flow on the time scales considered here. A detailed discussion of the evolving symmetric circulation of a translating vortex is presented elsewhere by Smith et al. (1995).

6 Vortex Tracks

Figure 3 shows the vortex tracks calculated numerically and analytically for the nine initial vortex positions. In broad terms, the agreement is very good, evidence that the theory captures the essential processes involved in the motion. For the initial vortex position NE, the difference between the two tracks is as small as 25 km after 48 hours. A similar result is obtained in the case SS (41 km), whereas for the position NW, the worst case, the difference between the vortex positions is 75 km after 24 hours and 296 km after 48 hours. The comparison suggests that the analytic theory provides an accurate representation of the vortex motion for at least 24 hours and can be used therefore to interpret the numerical calculations.

In general, the vortex track is determined by two effects, both of which are stronger west of the centre of deformation than in the east. Firstly, the symmetric vortex is simply advected by the initially-imposed large-scale flow. This advection depends strongly on the position of the vortex relative to the centre of flow deformation. For example, the eastward component of the large-scale flow reaches a strength of 8.33 ms^{-1} 1600 km west of the deformation field centre, but is only 0.24 ms^{-1} 600 km east of that point. Secondly, the initially symmetric vortex develops an asymmetry in the presence, *inter alia,* of a basic-state absolute vorticity gradient. The flow across the vortex centre associated with the azimuthal wavenumber-one component of this asymmetry gives an additional contribution to the motion. The analytic theory shows that the main contribution to this component is proportional to $|\nabla(\bar{\zeta} + f)|$, whereupon the asymmetry is largest in the region where $|\nabla(\bar{\zeta} + f)|$ is largest, i.e., west of the centre of deformation. For all initial vortex positions shown in Figure 3, these two effects partly cancel each other, so that the speed $|\mathbf{c}|$ of the vortex centre relative to the stationary Rossby wave is smaller than the advection speed $|\bar{\mathbf{v}}(\mathbf{x}_c)|$. Figure 3 shows the two effects separately for the initial vortex position SS.

The analytically-determined tracks deviate less from the corresponding numerical results if the vortex motion is slower, because the linearization of the environmental flow about the initial vortex position remains an accurate approximation for a longer period of time. As expected from the scale analysis, the analytic theory progressively breaks down if the wavelength of the Rossby wave is reduced. Then, the variation of the absolute vorticity gradient

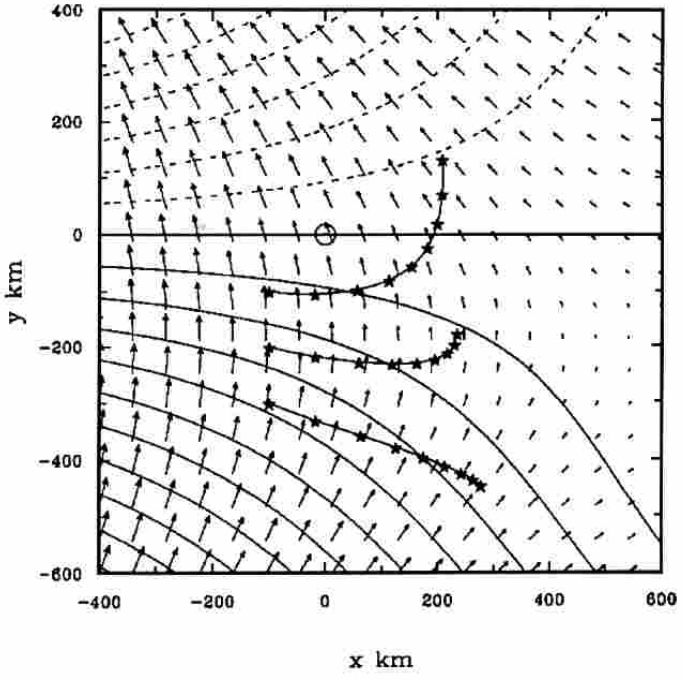

Figure 4 Vortex tracks calculated numerically with the initial vortex positions 100 km west and 100 km, 200 km, and 300 km south of the deformation field centre, denoted by the circle on the abscissa. The star symbols denote the vortex centre position every 12 hours. Solid (positive) and dashed lines (negative) are streamfunctions of the planetary-wave field; the contour interval is 1×10^6 m^2 s^{-1}. Small arrows represent the absolute vorticity gradient $\nabla(\bar{\zeta} + f)$, where the length of the vector is proportional to $|\nabla(\bar{\zeta} + f)|$.

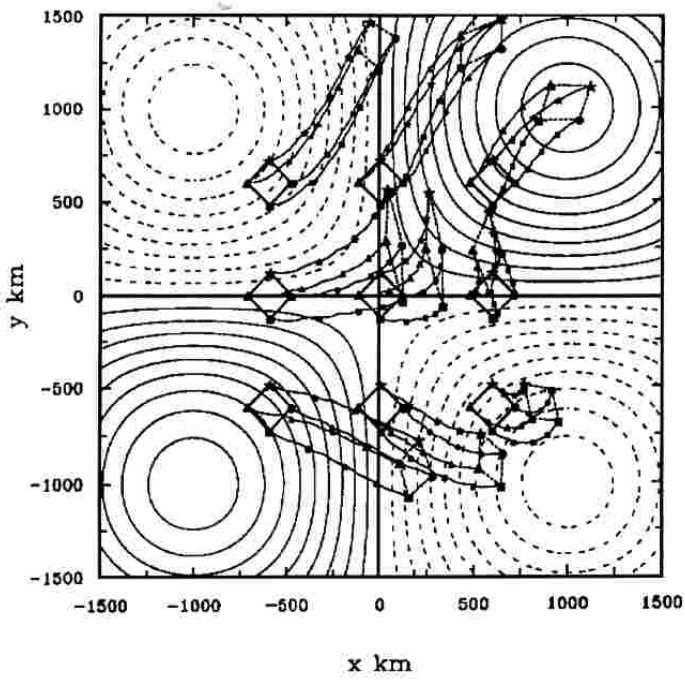

Figure 5 Vortex tracks calculated numerically for initial vortex positions 120 km west (triangle symbols), 120 km east (circle symbols), 120 km north (star symbols), and 120 km south (square symbols) of the nine positions defined in Figure 1. The symbols denote the vortex centre position every 12 hours. Solid (positive) and dashed lines (negative) are isolines of the Laplacian $\nabla^2(\bar{\zeta} + f)$ of the large-scale absolute vorticity; the contour interval is 2×10^{-18} m^{-2} s^{-1}.

$|\nabla(\bar{\zeta} + f)|$ is no longer small over the scale of the vortex and nonlinear interactions between the various wavenumber components become important.

The vortex tracks were calculated also with the maximum amplitude of the Rossby wave reduced to 3 ms^{-1}. These calculations gave a similar pattern of tracks to that shown in Figure 3, but the vortex motion was slower, mainly because of the decreased constant eastward flow component $\hat{U}$ of the Rossby wave. In particular for the initial vortex positions WW, NW, SU, and NN, a smaller difference between the numerically and analytically determined vortex tracks was obtained.

If the vortex motion were determined by advection only, the line of contraction of the deformation field could be expected to be a line along which the subsequent vortex motion has a certain sensitivity. Vortices initialized a fraction to the north of this line would subsequently track polewards, while those initially a fraction to the south would subsequently track equatorwards. It is evident that the existence of such lines (or regions) of sensitivity vis-à-vis the subsequent vortex motion have important implications for forecasting tropical cyclones whose initial positions are always inaccurate to some degree. In the present model calculations, the line of sensitivity is shifted equatorwards on account of the contribution to the vortex motion from the vortex asymmetry. This is illustrated in Figure 4 which shows the tracks of three vortices initialized 100 km, 200 km and 300 km to the south of the axis of contraction of the deformation field. Note that the first two eventually track polewards, while only the third one tracks equatorwards.

DeMaria (1985) conjectured that vortex tracks starting at different initial positions should diverge when the vector field of the absolute vorticity gradient $\nabla(\bar{\zeta} + f)$ is divergent, $\nabla^2(\bar{\zeta} + f) > 0$, while the opposite is true when $\nabla(\bar{\zeta} + f)$ is convergent, $\nabla^2(\bar{\zeta} + f) > 0$. This is easy to understand if the absolute vorticity gradient of the large-scale flow varies meridionally only and increases towards the north. Then, the northwestward component of the motion is stronger, the further north the initial vortex is located. Because of this, a vortex starting at a particular latitude lies always in a region of larger $|\nabla(\bar{\zeta} + f)|$ than one starting to the south of it

and hence, the speed of its motion is larger. As a consequence, the tracks of these two vortices diverge. In the present large-scale environment, $\nabla(\bar{\zeta} + f)$ varies in orientation and $\mathbf{j} \cdot \nabla(\bar{\zeta} + f)$, is negative to the northwest and southeast of the deformation field centre and positive to the northeast and southwest of that point (Here $\mathbf{j} = (0, 1, 0)$ is the unit vector pointing northwards). At the present level of approximation, the analytic theory cannot confirm or refute DeMaria's conjecture because the large-scale field is expanded in a Taylor series about the initial vortex position in a way that the absolute vorticity varies linearly about this point so that the Laplacian $\nabla^2(\bar{\zeta} + f)$ is zero. In principle, one can extend the analytic theory by taking higher-order terms in the Taylor-series expansion A1, but the algebraic complexity of this approach appears to obscure any obvious insights. Thus, numerical calculations were carried out to examine the behaviour of sets of tracks starting at points 120 km north, south, east, and west of the nine initial vortex positions considered before. These sets of vortex tracks are shown in Figure 5. Except for the tracks starting close to the position EE, it is evident that advection by the large-scale flow plays a major role for the vortex motion. None of the four tracks starting close to the positions NE and SW diverge, neither do those starting close to the positions NW and SE converge. However, significant divergence of the tracks occurs near the position WW, and convergence near the position EE, even though $|\nabla(\bar{\zeta} + f)|$ is equal to zero at these locations. Furthermore, the meridional divergence is largest and the zonal convergence smallest close to the deformation field centre, a region where $|\nabla(\bar{\zeta} + f)|$ is smallest, but where the stretching deformation is largest. These calculations would suggest that DeMaria's conjecture is at most a higher-order effect in the present flow configuration, consistent with it being absent at first- and second-order in the analytic theory.

7 Conclusions

A combined analytic and numerical study of tropical cyclone motion in a barotropic model on a beta-plane has been carried out for the case where the large-scale environmental flow varies zonally as well as meridionally. This flow has regions of significant stretching deformation whose effect on vortex motion has not been studied hitherto. An understanding of vortex motion in such regions is relevant to the initialization of tropical cyclones in numerical forecast models, because such regions exist in general flows and vortex tracks there may be sensitive to the initial vortex position.

The analytic theory is an extension of that developed by the second author for simpler large-scale flows and is derived on the basis of a power-series expansion in a small parameter ε characterizing the magnitude of the local absolute vorticity gradient of the environment. Since for a time period of 48 hours, the asymmetric vorticity patterns and vortex tracks agree acceptably well with those obtained from the numerical calculations, one can be confident that the analytic theory captures the essential features of the flow evolution during this time interval. Ultimately, the theory breaks down as nonlinear interactions between the various wavenumber components of the vortex asymmetry become important.

Some aspects of the evolution and subsequent motion of an initially symmetric vortex are similar to those in the case of a zonal shear flow. The vortex develops an asymmetry whose associated streamfunction pattern consists of a pair of counter-rotating gyres, analogous to the beta-gyres in the absence of a large-scale flow. At first order in the analytic theory, the vorticity asymmetry has entirely an azimuthal wavenumber-one structure, the strength and orientation of which are proportional to the strength and orientation of the local large-scale absolute vorticity gradient. The advection of vortex vorticity by the large-scale flow contributes to the vorticity asymmetry at second-order, where the main contribution is of azimuthal wavenumber-two and smaller ones are of wavenumbers-one and -three. The strength and orientation of the wavenumber-two component are proportional to the local strength and orientation of the total deformation flow, respectively, but the vortex motion is unaffected directly by this component. However, the patterns of advection associated with stretching deformation can have important implications for the track sensitivity to the initial vortex position as summarized below.

If the vortex motion in a large-scale flow in which there is appreciable stretching deformation were attributable to advection by the large-scale flow only, the axis of contraction of the deformation field would define a set of locations near which the subsequent vortex motion is sensitive to the initial vortex position. However, the presence of a large-scale absolute vorticity gradient and the consequent development of the vortex asymmetry change this simple picture. The calculations presented here show that the region of sensitivity still occurs, but is

shifted relative to the axis of deformation. The sensitivity with respect to the initial vortex position where the Laplacian of the large-scale absolute vorticity gradient is positive, as conjectured by DeMaria, is at most a higher-order effect in the large-scale flow studied here.

Acknowledgements

We thank Dr. Michael Reeder of Monash University for his comments on the original manuscript. This work was supported by the US Office of Naval Research through grant No. N00014-90-J-1487.

Appendix

(a) Series Expansion for the Environmental Flow

The environmental flow in the neighbourhood of the moving vortex may be obtained from a Taylor series expansion about the initial vortex centre of the corresponding flow defined in the fixed frame, i.e.,

$$\begin{aligned}\overline{\mathbf{u}}(\mathbf{X},t) \approx\ & \overline{\mathbf{u}}|_{\mathbf{X}=-\mathbf{x}_c} + (\mathbf{X}+\mathbf{x}_c)\cdot\nabla\overline{\mathbf{v}}|_{\mathbf{x}=\mathbf{0}} \\ & + \frac{1}{2}X^2\frac{\partial^2\overline{\mathbf{v}}}{\partial x^2}\bigg|_{\mathbf{x}=\mathbf{0}} + XY\frac{\partial^2\overline{\mathbf{v}}}{\partial x\,\partial y}\bigg|_{\mathbf{x}=\mathbf{0}} + \\ & + \frac{1}{2}Y^2\frac{\partial^2\overline{\mathbf{v}}}{\partial y^2}\bigg|_{\mathbf{x}=\mathbf{0}} \\ & + Xx_c\frac{\partial^2\overline{\mathbf{v}}}{\partial x^2}\bigg|_{\mathbf{x}=\mathbf{0}} + (Xy_c + Yx_c)\frac{\partial^2\overline{\mathbf{v}}}{\partial x\,\partial y}\bigg|_{\mathbf{x}=\mathbf{0}} + \\ & + Yy_c\frac{\partial^2\overline{\mathbf{v}}}{\partial y^2}\bigg|_{\mathbf{x}=\mathbf{0}}.\end{aligned} \tag{A1}$$

Clearly the accuracy of this approximation depends on the magnitude of vortex displacements in comparison with the scale of local gradients in the flow. The comparison between the analytically and numerically calculated vortex tracks in Figure 3 shows it to be a useful approximation in the present problem.

(b) Approximation of the Advection Operator $\overline{\mathbf{u}}\cdot\nabla$

Writing Eq. (A1) in terms of $\overline{D}$, $\overline{\zeta}$, $\overline{E}$ and $\overline{F}$, with each of these terms evaluated at the initial vortex centre in the fixed frame of reference, the differential operator $\overline{\mathbf{u}}\cdot\nabla$ takes the form

$$\begin{aligned}\overline{\mathbf{u}}\cdot\nabla = & \left[\frac{r}{2}(D + x_c\overline{D}_x + y_c\overline{D}_y)\right. \\ & + \frac{r^2}{16}(5\overline{D}_x + \overline{E}_x + \overline{F}_y - \overline{\zeta}_y)\cos\varphi + \\ & \quad + \frac{r^2}{16}(5\overline{D}_y - \overline{E}_y + \overline{F}_x + \overline{\zeta}_x)\sin\varphi \\ & + \frac{r}{2}(E + x_c\overline{E}_x + y_c\overline{E}_y)\cos 2\varphi + \\ & \quad + \frac{r}{2}(F + x_c\overline{F}_x + y_c\overline{F}_y)\sin 2\varphi \\ & \left. + \frac{r^2}{8}(\overline{E}_x - \overline{F}_y)\cos 3\varphi + \frac{r^2}{8}(\overline{F}_x + \overline{E}_y)\sin 3\varphi\right]\frac{\partial}{\partial r} \\ & + \left[\frac{r}{2}(\zeta + x_c\overline{\zeta}_x + y_c\overline{\zeta}_y)\right. \\ & + \frac{r^2}{16}(5\overline{\zeta}_x + \overline{F}_x + \overline{D}_y - \overline{E}_y)\cos\varphi + \\ & \quad + \frac{r^2}{16}(5\overline{\zeta}_y - \overline{F}_y - \overline{D}_x - \overline{E}_x)\sin\varphi \\ & + \frac{r}{2}(F + x_c\overline{F}_x + y_c\overline{F}_y)\cos 2\varphi - \\ & \quad - \frac{r}{2}(E + x_c\overline{E}_x + y_c\overline{E}_y)\sin 2\varphi \\ & \left. + \frac{r^2}{8}(\overline{F}_x + \overline{E}_y)\cos 3\varphi - \frac{r^2}{8}(\overline{E}_x + \overline{F}_y)\sin 3\varphi\right]\frac{1}{r}\frac{\partial}{\partial\varphi}\end{aligned}$$

where, for example, $\overline{D}_x$ denotes $\partial\overline{D}/\partial x|_{\mathbf{x}=\mathbf{0}}$. Since only the contributions to the vorticity asymmetry relative to the vortex centre are of interest, there is no need to take into account the spatially uniform terms $\overline{\mathbf{u}}(\mathbf{X}=\mathbf{x},t)$ and $\mathbf{x}_c\cdot\nabla\overline{\mathbf{v}}(\mathbf{x}=\mathbf{0})$;

(c) Expressions for $\zeta'_{241n}(r,t)$, $\zeta'_{242xn}(r,t)$, *and* $\zeta'_{243n}(r,t)$

The expressions for ζ'_{241n} and ζ'_{243n} are

$$\zeta'_{241c}(r,t) = -\frac{r^2}{16}\frac{d\zeta_v}{dr}\left(\frac{\sin(\Omega_r t)}{\Omega_r}(\overline{E}_x - \overline{\zeta}_y) - \frac{1-\cos(\Omega_r t)}{\Omega_r}(\overline{\zeta}_x - \overline{E}_y)\right),$$

$$\zeta'_{241s}(r,t) = -\frac{r^2}{16}\frac{d\zeta_v}{dr}\left(\frac{1-\cos(\Omega_r t)}{\Omega_r}(\overline{E}_x - \overline{\zeta}_y) + \frac{\sin(\Omega_r t)}{\Omega_r}(\overline{E}_x - \overline{\zeta}_y)\right),$$

$$\zeta'_{243c}(r,t) = -\frac{r^2}{8}\frac{d\zeta_v}{dr}\left(\frac{\sin(3\Omega_r t)}{3\Omega_r}\overline{E}_x - \frac{1-\cos(3\Omega_r t)}{3\Omega_r}\overline{E}_y\right),$$

$$\zeta'_{243s}(r,t) = -\frac{r^2}{8}\frac{d\zeta_v}{dr}\left(\frac{1-\cos(3\Omega_r t)}{3\Omega_r}\overline{E}_x + \frac{\sin(3\Omega_r t)}{3\Omega_r}\overline{E}_y\right).$$

The contribution to $\mathbf{x_c}$ associated with the first-order vorticity asymmetry is given in Footnote 1, while the contribution associated with the deformation field is approximated by

$$x_c(t) \approx \overline{u}(\mathbf{x}=\mathbf{0})\cdot t \equiv \overline{u}_c \cdot t$$

and

$$y_c(t) \approx \overline{v}(\mathbf{x}=\mathbf{0})\cdot t \equiv \overline{v}_c \cdot t.$$

Then, the expressions $\zeta'_{242xc}(r,t)$ and $\zeta'_{242xs}(r,t)$ take the form

$$\zeta'_{242xc}(r,t) = r\frac{d\zeta_v}{dr}\frac{B_*}{4}(\overline{E}_x\cos\varphi_* - \overline{E}_y\sin\varphi_*) \times \int_0^\infty \rho\left[\left(\frac{1}{4\Omega_r^2}\frac{\cos(\Omega_\rho t)}{4\Omega_r^2-\Omega_\rho^2} + \frac{\Omega_\rho^2}{4\Omega_\rho^2}\frac{\cos(2\Omega_r t)}{4\Omega_r^2-\Omega_\rho^2}\right)\cos 2\varphi + \left(\frac{t}{2\Omega_r} - \frac{2\Omega_r}{\Omega_\rho}\frac{\sin(\Omega_\rho t)}{4\Omega_r^2-\Omega_\rho^2} + \frac{\Omega_\rho^2}{4\Omega_r^2}\frac{\sin(2\Omega_r t)}{4\Omega_r^2-\Omega_\rho^2}\right)\sin 2\varphi\right]d\rho - \frac{r}{2}\frac{d\zeta_v}{dr}(\overline{u}_c\overline{E}_x + \overline{v}_c\overline{E}_y)\frac{1-\cos(2\Omega_r t)}{4\Omega_r^2},$$

$$\zeta'_{242xs}(r,t) = -r\frac{d\zeta_v}{dr}\frac{B_*}{4}(\overline{E}_y\cos\varphi_* + \overline{E}_x\sin\varphi_*) \times \int_0^\infty \rho\left[\left(\frac{\sin(\Omega_\rho t)}{4\Omega_r^2-\Omega_\rho^2} - \frac{\Omega_\rho}{2\Omega_r}\frac{\sin(2\Omega_r t)}{4\Omega_r^2-\Omega_\rho^2}\right)\cos 2\varphi + \left(\frac{1}{2\Omega_r\Omega_\rho} - \frac{2\Omega_r}{\Omega_\rho}\frac{\cos(\Omega_\rho t)}{4\Omega_r^2-\Omega_\rho^2} + \frac{\Omega_\rho}{2\Omega_r}\frac{\cos(2\Omega_r t)}{4\Omega_r^2-\Omega_\rho^2}\right)\sin 2\varphi\right]d\rho - \frac{r}{2}\frac{d\zeta_v}{dr}(\overline{u}_c\overline{E}_x + \overline{v}_c\overline{E}_y)\frac{2\Omega_r t - \sin(2\Omega_r t)}{4\Omega_r^2}$$

References

Chan, J. C. and *R. T. Williams,* 1987: Analytical and numerical studies of the beta-effect in tropical cyclone motion. Part I: Zero mean flow. J. Atmos. Sci. **44**, 1257–1265.

DeMaria, M., 1985: Tropical cyclone motion in a nondivergent barotropic model. Mon. Wea. Rev. **113**, 1199–1210.

Fiorino, M. and *R. L. Elsberry,* 1989: Some aspects of vortex structure related to tropical cyclone motion. J. Atmos. Sci. **46**, 975–990.

Hellmeier, A., 1993: The barotropic dynamics of tropical cyclone motion in a large-scale deformation field. Diplom dissertation, University of Munich, 77 pp.

Kasahara, A. and *G.W. Platzman,* 1963: Interaction of a hurricane with a steering field and its effect upon the hurricane trajectory. Tellus **15**, 321–335.

Peng, M. S. and *R. T. Williams,* 1990: Dynamics of vortex asymmetries and their influence on vortex motion on a beta-plane. J. Atmos. Sci. **47**, 1987–2002.

Ross, R. J. and *Y. Kurihara,* 1992: A simplified scheme to simulate asymmetries due to the beta effect in barotropic vortices. J. Atmos. Sci. **49**, 1620–1628.

Shapiro, L. J. and *K. V. Ooyama,* 1990: Barotropic vortex evolution on a beta plane. J. Atmos. Sci. **47**, 170–187.

Smith, R. K. and *W. Ulrich,* 1990: An analytical theory of tropical cyclone motion using a barotropic model. J. Atmos. Sci. **47**, 1973–1986.

Smith, R. K., W. Ulrich and *G. Dietachmayer,* 1990: A numerical study of tropical cyclone motion using a barotropic model. Part I: The role of vortex asymmetries. Quart. J. Meteor. Soc. **116**, 337–362.

Smith, R. K., 1991: An analytic theory of tropical cyclone motion in a barotropic shear flow. Quart. J. Meteor. Soc. **117**, 685–714.

Smith, R. K. and *W. Ulrich,* 1993: Vortex motion in relation to the absolute vorticity gradient of the vortex environment. Quart. J. Meteor. Soc. **119**, 207–215.

Smith, R. K. and *H. C. Weber,* 1993: An extended analytic theory of tropical cyclone motion in a barotropic shear flow. Quart. J. Meteor. Soc. **119**, 1149–1166.

Smith, R. K., 1993: On the theory of tropical cyclone motion. In 'Tropical Cyclone Disasters', Ed. Lighthill et al., Peking University Press, Beijing, 264–279.

Smith, R. K., H. C. Weber and *A. B. Kraus,* 1995: On the symmetric circulation of a moving hurricane. Quart. J. Meteor. Soc. **121**, (in press).

Ulrich, W. and *R. K. Smith,* 1991: A numerical study of tropical cyclone motion using a barotropic model. Part II: Motion in spatially-varying large-scale flows. Quart. J. Meteor. Soc. **117**, 107–124.